

Thermodynamics of a Dense Self-Avoiding Walk with Contact Interactions

A. M. Nemirovsky,¹ Jacek Dudowicz,¹ and Karl F. Freed¹

Received July 2, 1991

A lattice model is used to study the properties of an infinite self-avoiding linear polymer chain that occupies a fraction Φ , $0 \leq \Phi \leq 1$, of sites on a d -dimensional hypercubic lattice. The model introduces an (attractive or repulsive) interaction energy ε between nonbonded monomers that are nearest neighbors on the lattice. The lattice cluster theory enables us to derive a double series expansion in ε and d^{-1} for the chain free energy per segment while retaining the full Φ dependence. Thermodynamic quantities, such as the entropy, energy, and mean number of contacts per segment, are evaluated, and their dependences on Φ , ε , and d are discussed. The results are in good accordance with known limiting cases.

KEY WORDS: Self-avoiding walk; self-interacting walk; dense walk; lattice model of polymers; polymer packing; connectivity constant.

1. INTRODUCTION

Many interesting theoretical questions have been generated by studying the properties of macromolecules in concentrated solutions, melts, and the solid state. A great deal of work in this area has involved the development of several polymer models.^(1,2) In particular, the lattice model of polymers has been quite successful in predicting many thermodynamic properties of macromolecular fluids and glasses.^(1,2) The lattice model describes a flexible polymer as a self-avoiding random walk on a regular lattice of N sites as illustrated in Fig. 1. The walk is a succession of $M - 1$ steps (bonds) joining M consecutive sites (monomers). Excluded-volume constraints prohibit multiple occupancy of sites. M is the polymerization index and is propor-

¹ James Franck Institute, University of Chicago, Chicago, Illinois 60637.

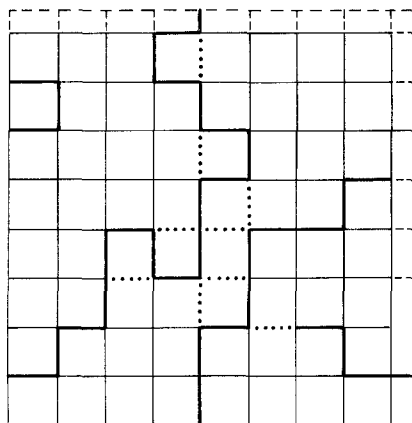


Fig. 1. Typical configuration of a self-interacting SAW filling a fraction $\Phi = M/N$ on a square lattice of N sites. M is the number of sites (proportional to the molecular weight) occupied by the walk. Nearest neighbor sites that are not consecutive along the chain (indicated by dotted lines connecting both sites) interact with a contact energy ε . Periodic boundary conditions are assumed along all directions.

tional to the molecular weight. Our interest here lies in the single-chain thermodynamic limit of

$$N \rightarrow \infty, \quad M \rightarrow \infty, \quad 0 \leq \Phi = M/N \leq 1 \quad (1)$$

with Φ the polymer packing fraction. A dense (dilute) walk has $\Phi > 0$ ($\Phi = 0$).

A widely used generalization of the self-avoiding lattice model introduced by Orr⁽³⁾ incorporates the van der Waals monomer–monomer interaction as follows: Two nearest neighbor nonbonded monomers interact with an energy ε . These interactions are represented in Fig. 1 by dotted lines. Van der Waals interactions generally produce attractive energies ($\varepsilon < 0$). As ε increases in absolute value, a dilute solution ($\Phi = 0$) chain contracts. When ε reaches some critical value ε_θ (the Flory θ point) the effects of the repulsive (excluded-volume) and attractive interactions cancel to a large extent. For more negative ε the chain collapses into a condensed state (the collapse transition). Positive ε corresponds to enhanced repulsion between neighboring nonsequential monomers, and a neighbor-avoiding walk (NAW) is obtained in the $\varepsilon \rightarrow \infty$ limit.

The connectivity constant μ [$\mu = \exp(-f)$, with f the dimensionless free energy per segment] is one of the most studied quantities in the vast literature on self-avoiding walks (SAWs), although *only particular limiting cases have been previously considered*. In particular, there are many studies of athermal ($\varepsilon = 0$) chains in the limits of infinite dilution⁽⁴⁻⁶⁾ ($\Phi = 0$) and

at full packing⁽⁷⁻¹⁰⁾ ($\Phi = 1$). Also, several researchers have considered the ε dependence of various dilute polymer properties.⁽¹¹⁻¹⁶⁾

The connectivity constant for athermal ($\varepsilon = 0$) self-avoiding chains at $\Phi = 0$ has been evaluated for various $d = 2$ and 3 regular lattices using directed enumeration techniques together with Padé approximants and extrapolations based on the ratio method.⁽⁴⁾ The best values for square and simple cubic lattices are $\mu_{\text{SAW}}^{\text{sq}} = 2.6385$ and $\mu_{\text{SAW}}^{\text{sc}} = 4.6835$, respectively.⁽⁴⁾ Some time ago, Fisher and Gaunt⁽⁵⁾ developed a d^{-1} expansion of μ for d -dimensional hypercubic lattices through fifth order in z^{-1} , with $z = 2d$ the lattice coordination number. The first terms of the series, which was later shown to be asymptotic,⁽⁶⁾ are⁽⁵⁾

$$\mu = z(1 - z^{-1} - z^{-2} + \dots), \quad z = 2d \quad (2)$$

The properties of dilute self-avoiding polymers ($\Phi = 0$) with nearest neighbor energies ε have been evaluated using direct enumeration and Monte Carlo techniques.⁽¹¹⁻¹⁶⁾ For instance, Fisher and Hiley⁽¹¹⁾ computed the free energy, internal energy, entropy, and mean number of contacts for a single chain as function of ε for square and simple cubic lattices. Rapaport⁽¹²⁾ studied self-interacting SAWs on an fcc lattice and analysed the ε dependence of μ for a wide range of attractive and repulsive ε . More recently, Ishinabe⁽¹³⁾ evaluated $\mu(\varepsilon)$ for SAWs on square and tetrahedral lattices over a range of energy about ε_{θ} . These studies⁽¹¹⁻¹⁶⁾ find that μ is a monotonically decreasing function of ε . This is easily understood since $-\ln \mu$, the free energy per monomer, grows as ε increases.

Dense ($\Phi > 0$) walks are used to model concentrated solutions of polymers, blends, melts and collapsed macromolecules.⁽⁷⁻¹⁰⁾ Hamiltonian walks (HW) produce the most compact packing of a single athermal SAW on a lattice, as all sites are occupied by monomers ($\Phi = 1$). The exact values of the HW connectivity constants are only known for a few special two-dimensional lattices. For example, Kasteleyn exactly determines the number of Hamiltonian walks on a Manhattan lattice, obtaining $\mu_{\text{hw}} = \exp(G/\pi)$, where G is the Catalan's constant.⁽⁷⁾ The best value of μ_{hw} for an square lattice ($\mu_{\text{hw}}^{\text{sq}} = 1.472$) has been obtained by Schmaltz *et al.*⁽⁸⁾ using strip methods. Orland *et al.*⁽⁹⁾ apply a field-theoretic representation of the packing problem to count the number of SAW configurations which fill a hypercubic lattice. Their d^{-1} expansion of μ_{hw} yields

$$\mu_{\text{hw}} = (z/e) + O(z^{-1}) \quad (3)$$

where the first term on the right-hand side is the mean field contribution. The one-loop contribution of $O(z^0)$ is found to vanish. Since Eq. (3) for $d = 2$ produces a value surprisingly close to that of Schmaltz *et al.*,⁽⁸⁾ Orland *et al.*⁽⁹⁾ raised the possibility that higher corrections to mean field from fluctuations might vanish to all orders.

Dense athermal walks have recently been studied with a variety of techniques. Duplantier and Saleur⁽¹⁰⁾ calculated the connectivity constant μ as a function of Φ , $0 \leq \Phi \leq 1$, for a single athermal $\varepsilon = 0$ chain on a square lattice using transfer matrix methods. Their values at $\Phi = 0$ and $\Phi = 1$ are very close those of refs. 4 and 8, respectively. Nemirovsky and Coutinho-Filho⁽¹⁷⁾ employed field-theoretic techniques to obtain the Φ -dependent connectivity constant of athermal chains as a series in powers of d^{-1} . The infinite-dilution limit of the series in ref. 17 agrees with (2), while at full packing it reproduces (3). In addition, ref. 17 shows that the next term of the series in $d = z/2$ for μ_{hw} is nonvanishing, contrary to the expectations of ref. 9. Moreover, at $d = 2$ the results of ref. 17 are in good agreement with those of ref. 10 over the whole range $0 \leq \Phi \leq 1$.²

The lattice cluster theory^(18,19) (LCT) has been developed extensively by Freed and co-workers to study a variety of thermodynamic properties of dense polymer solutions, melts, and blends. This theory also considers the Orr model on a d -dimensional hypercubic lattice, and produces $1/d$ expansions for thermodynamic properties. The LCT begins with an exact representation of the chain partition function and then expands it about a zeroth-order Flory approximation (which is exact at $d = \infty$). Previous work^(18,19) focuses on the many-chain thermodynamic limit of M finite and

$$N \rightarrow \infty, \quad p \rightarrow \infty, \quad 0 < \Phi = pM/N \leq 1 \quad (4)$$

with p the number of chains. On the other hand, ref. 17 uses the field-theoretic form of the LCT to study the limit of (1) for a single dense walk. These methods produce an alternative derivation of the z^{-1} expansion for the free energy or other quantities of interest. However, ref. 17 treats only athermal chains.

Here we consider a single flexible self-avoiding polymer of molecular weight M and nearest neighbor interaction ε such that the chain fills a non-zero fraction of a d -dimensional hypercubic lattice. The LCT is generalized in Section 2 to describe the thermodynamic limit (1) of a single, dense self-interacting SAW. The free energy per segment is evaluated as a double series expansion in powers of both ε and d^{-1} retaining the full dependence on the packing fraction Φ . Various thermodynamic properties of interacting dense walks, such as the internal energy, entropy, and mean number of contacts per segment, are calculated as functions of packing fraction, contact energy, and dimensionality. Section 3 discusses the results and compares them in some limiting cases with previous calculations. This is, to our knowledge, the first treatment of *self-interacting dense SAWs*.

²The corrected values of diagrams (e) and (i) in Table I of ref. 17 are $8M\Phi^2z^{-2/3}$ and $(-6M\Phi^2 + 2M\Phi^3)z^{-2}$, respectively.

2. LATTICE CLUSTER THEORY FOR AN INTERACTING SAW

This section briefly outlines the systematic computations of corrections to the mean field free energy for a single linear chain which occupies M lattice sites on a d -dimensional hypercubic lattice in the thermodynamic limit of (1). These corrections reflect the correlations between monomer positions that arise from chain connectivity and monomer interactions. According to the lattice cluster theory,⁽¹⁷⁻¹⁹⁾ the single-chain partition function can be written as

$$Z = Z^{\text{mf}}(1 + \text{corrections}) \tag{5}$$

where Z^{mf} is the mean field contribution and where entropic and energetic corrections are conveniently represented as an expansion in Mayer-like diagrams. The entropy diagrams contain various combinations of B correlating bonds, while the energy diagrams may have correlating bonds in addition to l interaction lines that join interacting monomers.⁽¹⁸⁾

The value of an individual diagram is the product of a lattice-structure-dependent generalized connectivity factor $D_{B,l}$ and a lattice-structure-independent combinatorial factor $\gamma_{D,l}$. Each interaction line additionally contributes a Mayer function $\exp(-\epsilon) - 1$ to $D_{B,l}$. In contrast to the general case of many interacting chains, where B correlating bonds may lie on different chains, only one-chain diagrams are allowed for the system under consideration.⁽¹⁷⁾ Examples of energy diagrams with one interaction line and with $B=1$ and $B=2$ bonds are given in Figs. 2 and 3, where crosses and circles are used to distinguish interacting from noninteracting monomers, respectively. Straight and curved lines designate correlating bonds and interaction lines, respectively. Diagrams $b_1, b_2,$ and b_3 of Fig. 2 are one-bond diagrams with, respectively, one disconnected, a singly connected, and a doubly connected interaction line. These three main combinations also appear in the remaining first-order energy diagrams of Fig. 2. Examples of second-order energy diagrams (with two interaction lines) containing up to $B=1$ correlating bonds are provided in Fig. 3. The

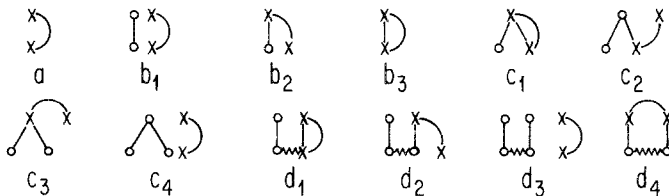


Fig. 2. First-order energy diagrams which contain one curved interaction line. Diagrams are given with up to $B=2$ correlating bonds (straight lines).

first two diagrams of Fig. 3 only have interaction lines that are connected sequentially (diagram a_1) and nonsequentially (diagram a_2). Thus, the interacting monomers in a_1 and a_2 are uncorrelated. There are no diagrams in Fig. 3 with two interaction lines between a pair of crossed vertices. Since the single-chain entropy diagrams (up to $B=4$ correlating bonds) are illustrated and evaluated in ref. 17, we focus here on the energy corrections to the partition function (5) which have not previously been calculated.

The evaluation of the connectivity factor $D_{B,l}$ for energy diagrams involves transforming the contributions from all interaction lines into the same form as that for correlating bonds. The calculations are performed in discrete Fourier space with \mathbf{q} the momentum variable. The main difference between the treatment of interaction lines and correlating bonds lies in the appearance of $\mathbf{q}=0$ contributions only for the former. However, as is proven in ref. 18, all $\mathbf{q}=0$ contributions may be ignored in all but the leading diagram a of Fig. 2, providing diagrams are multiplied by simple ε -dependent factors. The appropriate counting rules for both $\gamma_{D,l}$ and $D_{B,l}$ are described in detail in previous papers,^(18,19) so they are not discussed here.

The standard procedure of evaluating the Helmholtz free energy involves expansion of the logarithm of the right-hand side of (5) in a Taylor series. The resulting contributions with a given power of ε are then collected into cumulants. This process ensures cancellation of unphysical individual diagram contributions proportional to higher than the first power of M and finally leads to the representation of the free energy $F = -\ln Z$ as

$$f = F/M = -\ln Z/M = -s^{mf} - \sum_{B,l,i} (-1)^{\delta(1,0)} C_{B,l}^{(i)} - \varepsilon/kT \quad (6)$$

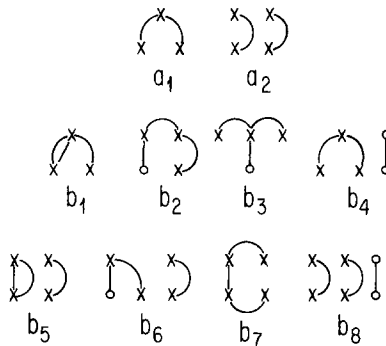


Fig. 3. Second-order energy diagrams with two interaction lines and up to $B=1$ correlating bonds.

where s^{mf} denotes the specific mean field entropy of a single SAW and $\delta(1, 0)$ is the Kronecker delta function. The sum over i in (6) means a sum over contributions from all cumulant diagrams $C_{B,l}^{(i)}$ with B correlating bonds and l interaction lines for all B and l . Computational details of $C_{B,l}^{(i)}$ will be presented elsewhere together with a full list of the cumulant diagrams through $B+l=4$ for arbitrary chain architectures.⁽²¹⁾ Since the lattice cluster theory formulation also includes interactions between bonded monomers, the term $-\varepsilon$ is introduced in (6) to eliminate this unwanted contribution. The $l=0$ cumulant diagrams $C_{B,l}^{(i)}$ reduce to the entropy diagrams $C_{B,0}^{(i)}$ evaluated in ref. 17. Diagrams $C_{0,l}$ having only interaction lines are called extended mean field diagrams to emphasize the absence of bonding-induced correlations in these terms.

After introducing the mean field entropy s^{mf}

$$s^{\text{mf}} = \ln(z/e) - (1 - \Phi)\Phi \ln(1 - \Phi) \quad (7)$$

and substituting the cumulant diagram corrections (up to $B+l=4$), the specific free energy (6) takes the form of a double series expansion in the inverse lattice coordination number z^{-1} and the dimensionless interaction energy ε (in units of kT). The result is written in the thermodynamic limit (1) as

$$f = f^{\text{mf}} + f^{\text{emf}} + f^{(1)} + f^{(2)} + \dots \quad (8)$$

with

$$f^{\text{mf}} = -\ln z + 1 + (1 - \Phi)\Phi^{-1} \ln(1 - \Phi) \quad (8a)$$

$$\begin{aligned} f^{\text{emf}} = & \varepsilon z \Phi / 2 - (\varepsilon^2 z) \Phi (1 - \Phi)^2 / 4 + (\varepsilon^3 z) \Phi (1 - \Phi)^2 \\ & \times (1 - 2\Phi)^2 / 12 - (\varepsilon^4 z) \Phi (1 - \Phi)^2 [1 - 6\Phi(1 - \Phi) \\ & \times (3\Phi^2 - 3\Phi + 2)] / 48 \end{aligned} \quad (8b)$$

$$\begin{aligned} f^{(1)} = & z^{-1} (1 - \Phi) - \varepsilon [1 - (1 - \Phi)^2] - \varepsilon^2 (1 - \Phi)^2 \Phi \\ & \times (1 - 7\Phi / 2 + 3\Phi^2) \end{aligned} \quad (8c)$$

$$\begin{aligned} f^{(2)} = & z^{-2} [3/2 - 3\Phi + (10/3)\Phi^2 - 2\Phi^3] + (\varepsilon z^{-1})(1 - \Phi)^2 \\ & \times (1 - 2\Phi + 4\Phi^2) \end{aligned} \quad (8d)$$

where superscripts mf and emf indicate the mean field and extended mean field approximations, and $f^{(1)}$ and $f^{(2)}$ denote the corrections to $f^{\text{mf}} + f^{\text{emf}}$ of order z^{-1} and z^{-2} , respectively. We employ the formal ordering of $\varepsilon \sim z^{-1}$. The leading extended mean field terms of order ε^3 and ε^4 are also included in f^{emf} . The expansion (8) is expected to be valid as long as z is large and $|\varepsilon| < z^{-1}$.

3. THERMODYNAMICS OF A SINGLE DENSE WALK

This section studies the thermodynamic properties of a single polymer chain as a function of the packing fraction Φ , the contact energy ε , and the dimensionality d . The free energy per segment given by (8) becomes simpler in the two interesting limiting cases of $\Phi=0$ (dilute chain) and $\Phi=1$ (Hamiltonian walk). Expanding f about $\Phi=0$ and retaining only the linear contribution in Φ produces

$$f(\Phi \approx 0) = f_{\text{dil}} + \Phi f'_{\text{dil}} + \dots \tag{9a}$$

$$f_{\text{dil}} = u_{\text{dil}} - s_{\text{dil}} = \varepsilon z^{-1} - (\ln z - z^{-1} - 3z^{-2}/2 + \dots) \tag{9b}$$

$$f'_{\text{dil}} = [\frac{1}{2} + \varepsilon z \exp(-\varepsilon)/2 - 2\varepsilon - \varepsilon^2 - 4\varepsilon z^{-1} - z^{-1} - 3z^{-2}] + \dots \tag{9c}$$

where $f_{\text{dil}} = f(\Phi=0)$, $f'_{\text{dil}} = df/d\Phi|_{\Phi=0}$, and the quantities u_{dil} and s_{dil} are, respectively, the energy and the entropy per segment of the dilute chain.

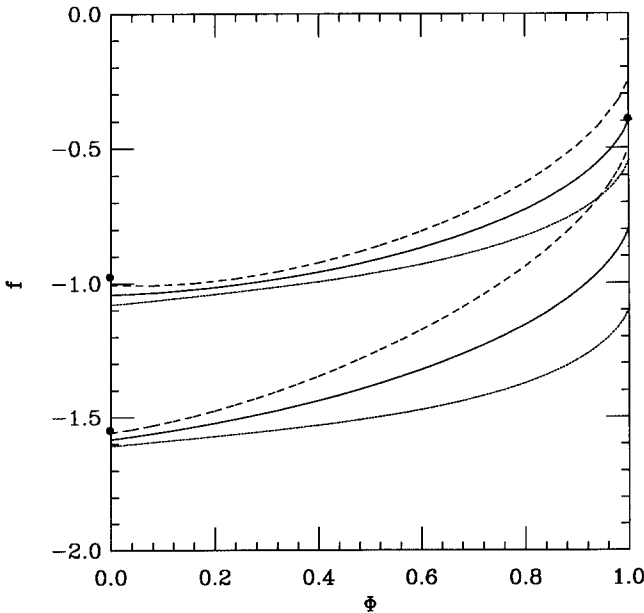


Fig. 4. Packing fraction dependence of the free energy per segment f for an interacting SAW on square ($z=4$ upper curves) and sc ($z=6$ lower curves) lattices. The athermal chain ($\varepsilon=0$) results are indicated by a solid line. Self-attracting (self-repelling) SAWs with $\varepsilon=-0.15$ ($\varepsilon=0.15$) produce the dotted (dashed) lines. The best available athermal chain values of f at $\Phi=0$ and $\Phi=1$ from refs. 4 and 8, respectively, are indicated by black dots.

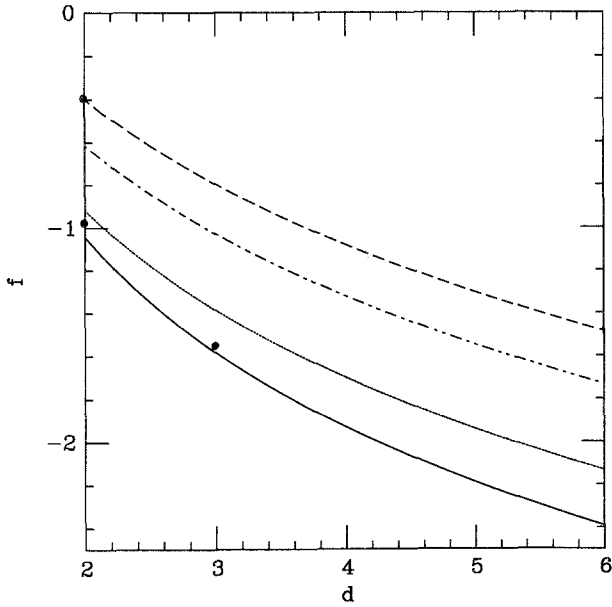


Fig. 5. Free energy per monomer versus dimensionality for athermal chains on d -dimensional hypercubic lattices. The packing fractions are $\Phi = 0$ (solid line), $\Phi = 0.5$ (dotted line), $\Phi = 0.9$ (dot-dashed line), and $\Phi = 1$ (dashed line). Black dots at $\Phi = 0$ and $\Phi = 1$ are from refs. 4 and 8, respectively.

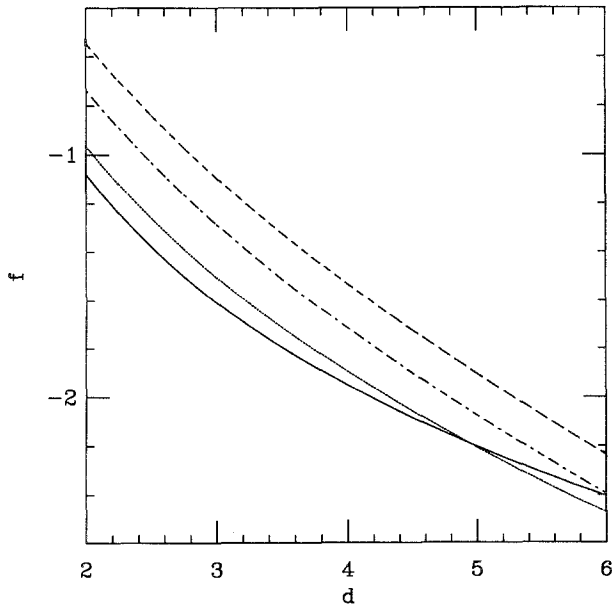


Fig. 6. Same as Fig. 5, but for self-attracting chains with $\epsilon = -0.15$.

Similarly, after expanding f of (8) about $\Phi = 1$ and keeping the linear term in $1 - \Phi$, we find

$$f(\Phi \approx 1) = f_{\text{hw}} + (1 - \Phi) f'_{\text{hw}} + \dots \quad (10a)$$

$$f_{\text{hw}} = u_{\text{hw}} - s_{\text{hw}} = (z - 2)\varepsilon/2 - [\ln(z/e) + z^{-2}/6 + \dots] \quad (10b)$$

$$f'_{\text{hw}} = -\varepsilon z/2 + \ln(1 - \Phi) + z^{-1} + 7z^{-2}/3 + \dots \quad (10c)$$

where the Hamiltonian walk entropy can be alternatively written as $s_{\text{hw}} = \ln \mu_{\text{hw}}$, with μ_{hw} the athermal Hamiltonian walk connectivity constant evaluated to $O(z^{-2})$ in ref. 17. This is because, as discussed below, the exact f_{hw} is linear in ε , and therefore s_{hw} is ε -independent.

Thermodynamic properties may now be obtained from the chain free energy per segment. For example, the mean number of contacts per monomer $\langle m \rangle$ is given by

$$\langle m \rangle = d(\ln f)/d\varepsilon \quad (11)$$

Inserting (10b) in (11) yields

$$\langle m \rangle_{\text{hw}} = (z - 2)/2 \quad (12)$$

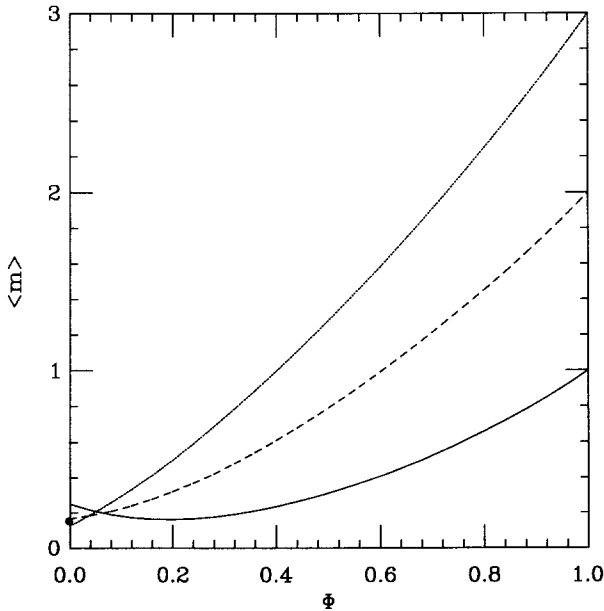


Fig. 7. Mean number of contacts per segment $\langle m \rangle$ as a function of Φ for an athermal dense walk on square (solid line), sc (dashed line), and 4-d hypercubic (dotted line) lattices. $\langle m \rangle$ is practically independent of ε for $|\varepsilon| < z^{-1}$. The $\Phi = 0$, $d = 2$ and $d = 3$ results from refs. 14 and 11, respectively, are indicated by superimposed black dots.

as contributions on $\langle m \rangle_{\text{hw}}$ only arise from f^{emf} and $f^{(1)}$. The second-order $f^{(2)}$ produces a vanishing contribution. We also expect that higher order contributions from $f^{(i)}$, $i > 2$, vanish since (12) is an *exact result*. In fact, it is easy to see that the maximum number of contacts per segment of a SAW on a d -dimensional hypercubic lattice is $d - 1$. This is also in accordance with previous^(3,11,14) discussions of the most compact packing of a self-avoiding chain. When the chains have $\Phi \approx 0$, use of (9) and (11) produces the interesting result

$$\langle m \rangle (\Phi \approx 0) = z^{-1} + \Phi(z/2 - 2 + \dots) + O(z^{-2}, \epsilon z^{-1}) \tag{13}$$

predicting that $\langle m \rangle \propto d^{-1}$ when $\Phi = 0$, but $\langle m \rangle \propto d$ when Φ is finite (dense walks). In fact, for infinite chains ($M \rightarrow \infty$), there is a *jump discontinuity* in $\langle m \rangle$ versus Φ at $\Phi = 0$ in the limit of $z \rightarrow \infty$ if Φ approaches zero slower than z^{-1} .

The internal energy u and entropy s per segment of the polymer chain are respectively obtained from

$$u = \langle m \rangle \epsilon \tag{14a}$$

$$s = -f + u \tag{14b}$$

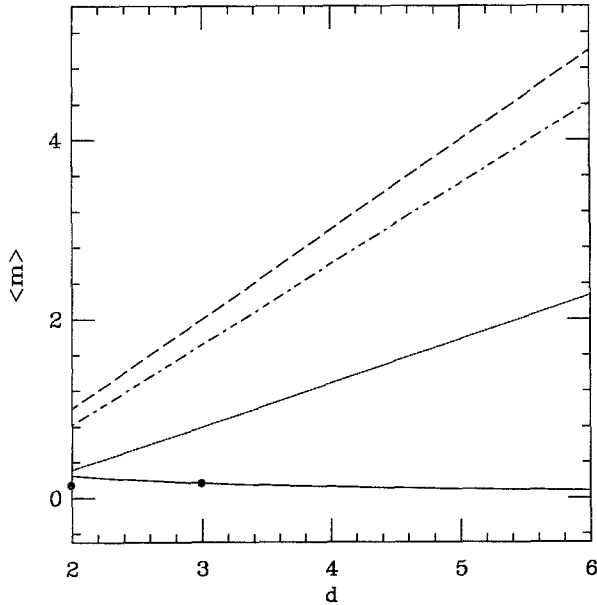


Fig. 8. The function $\langle m \rangle$ versus d for various packing fractions: $\Phi = 0$ (solid line), $\Phi = 0.5$ (dotted line), $\Phi = 0.9$ (dot-dashed line), and $\Phi = 1$ (dashed line). Black dots at $\Phi = 0$ are $\langle m \rangle_{\text{sq}} = 0.16$ and $\langle m \rangle_{\text{sc}} = 0.18$ from refs. 14 and 11, respectively.

and their values for infinitely dilute and densest walks are given by (9b) and (10b), respectively.

Figure 4 shows that the free energy per segment of a self-interacting infinite SAW is a monotonically increasing function of the packing fraction Φ , $0 \leq \Phi \leq 1$, for both, square ($z=4$) and sc ($z=6$) lattices. Also, f increases linearly with ε for $|\varepsilon| < z^{-1}$ for a given Φ and d . As discussed below, this occurs because the entropy per monomer is practically independent of ε , while the internal energy grows linearly with ε . The black dots for $\Phi=0$ and $\Phi=1$ in Fig. 4 indicate the best literature values^(4,8) for f in these limits.

The d dependence of f for athermal ($\varepsilon=0$) and self-attracting ($\varepsilon=-0.15$) chains is displayed in Figs. 5 and 6, respectively, for various Φ . Results for self-repulsive chains are similar to those for $\varepsilon=0$ but with larger separation between curves that differ in Φ . When $\varepsilon \geq 0$, f_{hw} at a fixed d provides an upper bound to the free energy per segment because Hamiltonian walks have the least specific entropy and the maximum number of contacts per segment. Hence, they have the largest internal energy. On the contrary, the internal energy of self-attractive walks is negative, so f_{hw} , which is an upper bound to f at low d , becomes a lower

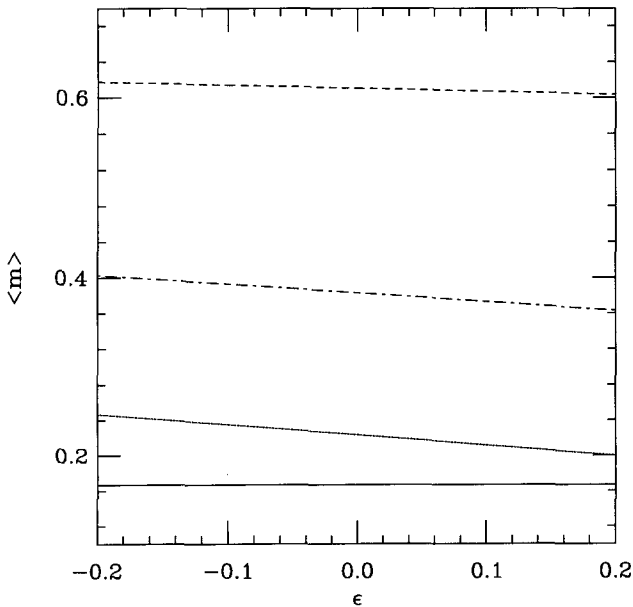


Fig. 9. The quantity $\langle m \rangle$ versus ε at various packing fractions: $\Phi=0$ (solid line), $\Phi=0.1$ (dotted line), $\Phi=0.25$ (dot-dashed line), and $\Phi=0.4$ (dashed line). The slope of the $\langle m \rangle$ vs. ε curves decreases as Φ approaches unity. $\langle m \rangle$ at $\Phi=1$ is ε -independent.

bound for large values of d . Therefore, as d grows, the curves for f versus d for different Φ become further apart for $\varepsilon \geq 0$ (Fig. 5) but approach (and ultimately cross) each other when $\varepsilon < 0$ (Fig. 6).

Figure 7 displays $\langle m \rangle$, the mean number of contacts per segment, as a function of Φ for square, sc, and $d=4$ hypercubic lattices. As expected, $\langle m \rangle$ grows as the packing is more compact. Although the calculated $\langle m \rangle$ for an square lattice appears to have a minimum at $\Phi \neq 0$ (which is absent for $d > 2$), we do not believe that this feature would persist in higher order calculations. In fact, our results improve as d , Φ , and ε grow. This is expected, since as fluctuations become less relevant at higher d and Φ , fewer corrections to mean field are required. Also, the predicted value $\langle m \rangle_{\text{dil}} = z^{-1} + O(z^{-2}, \varepsilon z^{-1})$ is substantially larger than those of refs. 11 and 14, which predict $0.16 < \langle m \rangle < 0.18$ for a square lattice. Since we expect $\langle m \rangle$ to grow with Φ , the value of our “minimum” could be taken as an upper bound to $\langle m \rangle$.

Figure 8 exhibits $\langle m \rangle$ as a function of d for various Φ . Dense (dilute) walks have the mean number of contacts per monomers grow (decrease) with dimensionality. [See Eq. (13).] For dense walks, this clearly arises

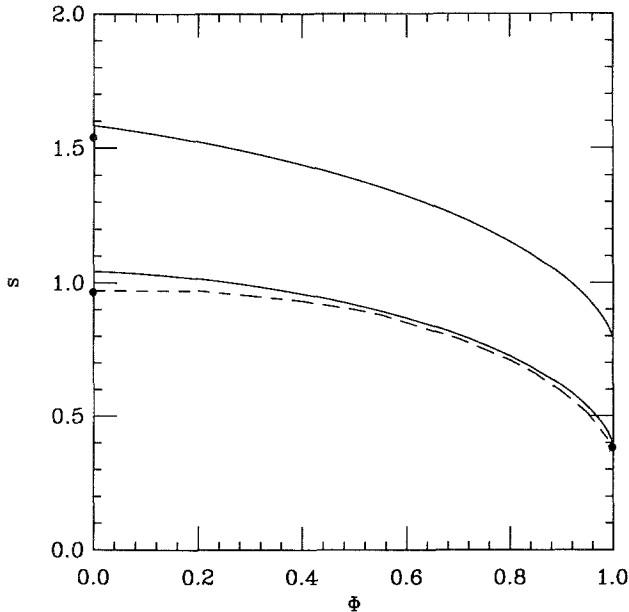


Fig. 10. The volume fraction dependence of the entropy per monomer for athermal chains on square (lower solid line) and sc (upper solid line) lattices. The dashed curve is from Duplantier and Saleur⁽¹⁰⁾ for square lattices. The best available results at $\Phi = 0$ and $\Phi = 1$ from refs. 4 and 8 are indicated by black dots.

because the higher the dimension (at fixed Φ), the larger is the number of nearest neighbor sites accessible to other monomers. A dilute walk with $\Phi = 0$, on the other hand, has more space available, and hence there is less chance of returning close to a previously visited site. $\langle m \rangle$ is a linearly decreasing function of ε for $|\varepsilon| < z^{-1}$, as illustrated in Fig. 9 for a self-interacting SAW on a sc lattice. Since $\langle m \rangle$ depends weakly on ε over the energy range considered, the chain internal energy of (14a) is then practically proportional to the contact energy.

The entropy per monomer is presented in Fig. 10 as a function of the polymer volume fraction for athermal chains on square and sc lattice. The entropy decreases from its maximum of s^{dil} at $\Phi = 0$ to its minimum value of $s_{\text{hw}} = \ln(z/e) + O(z^{-2})$ at $\Phi = 1$. The Duplantier and Saleur square lattice result for $0 \leq \Phi \leq 1$ is displayed for comparison. Ref. 17 provides other computations for athermal chains. The entropy per monomer has a very weak dependence on ε (about a 2–3% variation from its athermal limit) in the energy range considered here. For dense walks it always possesses a maximum at $\varepsilon = 0$. Figure 11 shows the d dependence of s for various Φ . As expected, the entropy per segment grows with d (as $\ln d$) because the

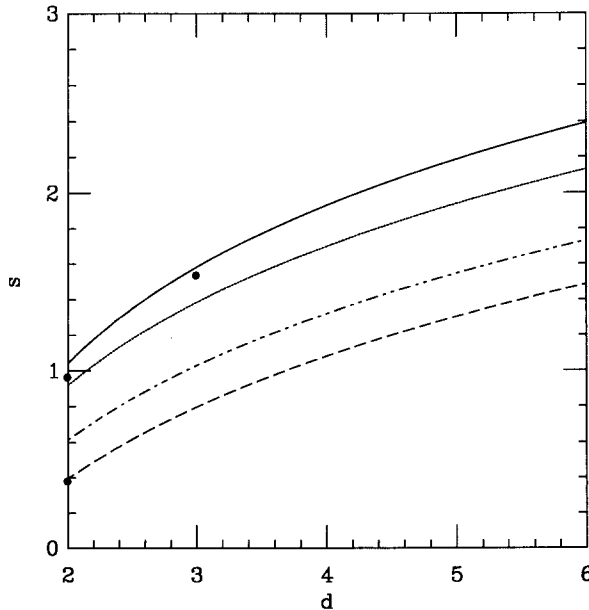


Fig. 11. The entropy per segment as a function of d for athermal dense walks at various packing fractions: $\Phi = 0$ (solid line), $\Phi = 0.5$ (dotted line), $\Phi = 0.9$ (dot-dashed line), and $\Phi = 1$ (dashed line). The entropy per segment changes very little with ε when $|\varepsilon| < z^{-1}$. Results of refs. 4 and 8 for dilute and the densest packing are indicated by black dots.

opening of space provides more configurational choices (growing as d) per monomer.

Let us now consider the $\Phi=0$ limit. We stress that, as briefly discussed above, our expansion becomes less reliable for small values of Φ and d and as the energies become more attractive. In fact, as fluctuations grow in importance (e.g., when $\Phi=0$ and $\varepsilon \leq 0$ in low d), more terms in the series expansion (8) are necessary and, in some instances, appropriate resummations may be required to produce good results. Hence, our present predictions for dilute walks are only semiquantitative. Figure 12 shows the free energy per monomer as a function of the contact energy ε for a dilute chain on square and sc lattices. Also presented are the $d=2$ and 3 results of Fisher and Hiley.⁽¹¹⁾ More recent predictions by Ishinabe⁽¹³⁾ of μ versus ε for a self-attracting SAW on a square lattice fall very close to those of ref. 11. Our results are quite reasonable for repulsive or weakly attractive SAWs. (Attractive walks with $\varepsilon < -z^{-1}$ lie beyond the range of validity for our expansion).

Although the $\Phi=0$ free energy per monomer of (9b) is in reasonable agreement with previous determinations, derivatives of this thermodynamic function are more sensitive to fluctuations, and hence higher order correc-

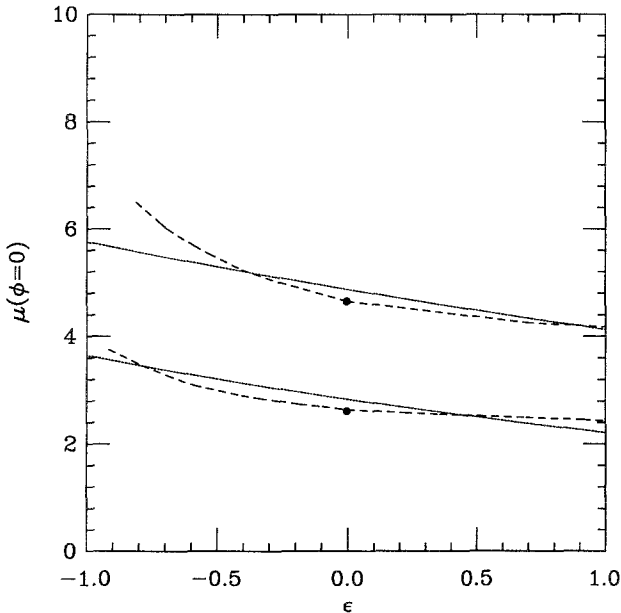


Fig. 12. The free energy per segment as a function of the contact energy ε for a self-interacting dilute ($\Phi=0$) walk on square (lower solid line) and sc (upper solid line) lattices. Results from Fisher and Hiley⁽¹¹⁾ are indicated by dashed lines. The black dots give the best value of the square and sc connectivity constant (μ at $\Phi=\varepsilon=0$).⁽⁴⁾

tions are required for other thermodynamic quantities. Because the calculated f_{dil} is linear in ε (to the order we evaluate), $\langle m \rangle_{\text{dil}}$ and s_{dil} are independent of the contact energy. On the other hand, refs. 11 and 12 show that the entropy per segment varies slowly with contact energy, exhibiting a maximum near $\varepsilon = 0$. Our predicted $s_{\text{dil}}(\varepsilon) = 1.03$ and 1.58 for square and sc lattices, respectively, are somewhat above that maximum entropy per monomer given in ref. 11. Also, our prediction $\langle m \rangle_{\text{dil}} = z^{-1}$ is about 50% larger than previous values for square and sc lattices.

4. CONCLUSIONS

This work investigates for first time dense self-interacting self-avoiding random walks on d -dimensional hypercubic lattices over the whole range $0 \leq \Phi \leq 1$ of polymer volume fractions. The lattice cluster theory (LCT) is used to evaluate the dense walk free energy per segment f in Eq. (8) as a function of the packing fraction Φ , the contact energy ε , and the dimensionality d of the space. Our d^{-1} expansion of f is valid as long as $|\varepsilon| < z^{-1}$, with $z = 2d$ the lattice coordination number. Higher order contributions may, in principle, be evaluated using the techniques of refs. 17–19 and references therein.

The important limiting cases of infinite dilution ($\Phi = 0$) and of the densest packing ($\Phi = 1$) are treated in some detail. When $\Phi \approx 0$, we find that the mean number of contacts per segment $\langle m \rangle$ of infinite chains has a jump discontinuity in the $z^{-1} \rightarrow 0$ limit when Φ approaches zero slower than z^{-1} . Hamiltonian walks ($\Phi = 1$) yield $\langle m \rangle_{\text{hw}} = d - 1$, in agreement with expectations. We also derive an expansion for f near full packing (i.e., about a HW with $\Phi \approx 1$). The predicted HW entropy per monomer for a square lattice is very close to its best literature values.

The interesting dependence of the free energy per segment, the entropy per monomer, and the mean number of contacts per monomer on volume fraction and dimensionality are discussed and compared with previous data in available limiting cases. This comparison and simple physical arguments indicate that our expansion is better at high packing fraction and dimensionality. This is because the LCT produces an expansion of the free energy or other quantities of interest about a Flory-type mean field which is exact at $d = \infty$. Since the fluctuations are added perturbatively, the smaller the fluctuations, the better is the mean field approximation, and the fewer are the corrections required to produce good results. Similar arguments indicate that our calculations are less reliable in the $\Phi = 0$ limit, and, in particular, when attractive contact interactions are present. Nevertheless, we find our $d = 2$ and 3 results for $\Phi = 0$ are in semiquantitative agreement with previous computations. Recent work⁽²¹⁾ combining the LCT with

exact enumerations produces an expansion of the $\Phi = 0$ free energy per monomer through fifth order in d^{-1} , retaining the full ε dependence. Ref. 21 investigates in depth this interesting $\Phi = 0$ regime.

Results of this paper strictly apply to hypercubic lattices. Other lattice types can also be studied similarly. Although the mean field approximation depends only on the coordination number z , corrections distinguish lattice types, such as hexagonal and sc, with the same z . This is in accordance with the conclusions of Bradley.⁽²²⁾ If we insist on using (10b) to obtain, for example, the connectivity constant of a Hamiltonian path on a Manhattan lattice (using $z = 3$), we find $\mu_{\text{hw}} = 1.11$, substantially lower than the exact⁽⁷⁾ $\mu_{\text{hw}} = 1.338\dots$ but better than the predictions of either the Flory-like theories ($\mu_{\text{hw}}^{\text{Flory}} = 0.74$) or that of Orland *et al.*⁽⁹⁾ ($\mu_{\text{hw}}^{\text{OID}} = 1.10$).

The LCT methods can be extended without difficulty to evaluate other polymer properties, such as mean size and critical exponents,⁽²¹⁾ and also to calculate thermodynamic functions of other interesting packing problems, such as self-avoiding surfaces. We are presently investigating the influence of polymer branching and structured monomers on the thermodynamic properties of dense walks.⁽²⁰⁾

ACKNOWLEDGMENTS

This research is supported in part by NSF Grant DMR 89-19941. We thank J. F. Douglas for useful discussion.

REFERENCES

1. H. Yamakawa, *Modern Theory of Polymer Solutions* (Harper & Row, New York, 1971); P. J. Flory, *Statistical Mechanics of Chain Molecules* (Wiley-Interscience, New York, 1969).
2. P. G. de Gennes, *Scaling Concepts in Polymer Physics* (Cornell University Press, Ithaca, New York, 1979); M. Doi and S. F. Edwards, *Theory of Polymer Dynamics* (Clarendon Press, Oxford, 1986); K. F. Freed, *Renormalization Group Theory of Macromolecules* (Wiley, New York, 1987).
3. W. J. C. Orr, *Trans. Faraday Soc.* **42**:12 (1946).
4. M. G. Watts, *J. Phys. A* **8**:61 (1975), and references therein.
5. M. E. Fisher and D. S. Gaunt, *Phys. Rev.* **133A**:224 (1964); M. E. Fisher, *Phys. Rev.* **162**:480 (1976).
6. P. R. Gerber and M. E. Fisher, *Phys. Rev.* **10**:4697 (1974).
7. P. W. Kasteleyn, *Physica* **29**:1329 (1963); P. D. Gujrati and M. Goldstein, *J. Chem. Phys.* **74**:2596 (1981); B. Duplantier and F. Douis, *J. Stat. Phys.* **51**:327 (1988).
8. T. G. Schmalz, G. E. Hite, and D. J. Klein, *J. Phys. A* **17**:445 (1984).
9. H. Orland, C. Itzykson, and C. de Dominicis, *J. Phys. Lett. (Paris)* **46**:353 (1985).
10. B. Duplantier and H. Saleur, *Nucl. Phys. B* **290**[FS20]:291 (1987).
11. M. E. Fisher and B. J. Hiley, *J. Chem. Phys.* **34**:1253 (1961).
12. D. C. Rapaport, *J. Phys. A* **9**:1521 (1976); **10**:637 (1977).

13. T. Ishinabe, *J. Phys. A* **18**:3181 (1985); **20**:6435 (1987).
14. T. Ishinabe and Y. Chikahisa, *J. Chem. Phys.* **85**:1009 (1986).
15. D. S. Gaunt, J. E. G. Lipson, J. L. Martin, M. F. Sykes, G. M. Torrie, S. G. Whittington, and M. K. Wilkinson, *J. Phys. A* **17**:211 [1984].
16. H. Meirovitch and H. A. Lim, *Phys. Rev. A* **39**:4186 (1989), and references therein; see also X.-F. Yuan and A. J. Masters, *J. Chem. Phys.* **94**:6908 (1991).
17. A. M. Nemirovsky and M. D. Coutinho-Filho, *J. Stat. Phys.* **53**:1139 (1988); *Phys. Rev. A* **39**:3120 (1989).
18. J. Dudowicz and K. F. Freed, *Macromolecules*, **24**:5076, 5112 (1991).
19. J. Dudowicz, K. F. Freed, and W. G. Madden, *Macromolecules* **23**:4803 (1990).
20. A. M. Nemirovsky, J. Dudowicz, and K. F. Freed, *Phys. Rev. A*, in press.
21. A. M. Nemirovsky, K. F. Freed, T. Ishinabe, and J. F. Douglas, *J. Stat. Phys.*, in press; *Phys. Lett. A*, in press.
22. R. M. Bradley, *J. Phys. A* **22**:L19 (1989).